Bonded Repairs of Composite Sandwich Structures: Impregnation Process and Quality Assessment

Jingcai Zhou[1,2], Pascal Hubert[1,2*]

[1] Structures and Composite Materials Laboratory, Department of Mechanical Engineering, McGill University, 817 rue Sherbrooke Ouest, MacDonald Building, Montreal, H3A 0C3, QC, Canada

[2] Centre de recherche sur les systèmes polymères et composites à haute performance (CREPEC) Montreal, Canada

* *Corresponding author (pascal.hubert@mcgill.ca)*

Keywords: *Composite Repair; Design of Experiment; Impregnation; Vacuum Bagging Arrangement; Void Formation*

1. Abstract

In recent years, carbon fibre reinforced polymer composites have increasingly replaced metallic materials in aircraft structures due to their high strength-to-weight ratio. Despite their superior mechanical properties, CFRP structures remain susceptible to damage during both manufacturing and in-service operations. When damage is not extensive, bonded repair techniques can be employed to restore airworthiness by optimizing bond strength and ensuring durability under varied operating environments. Although bonded repairs can provide significant strength recovery in composite structures, variability in processing factors poses challenges to achieving consistent repair quality. In this work, the repair patch quality is investigated by systematically varying process factors, such as impregnation method, bagging configuration, cure cycle. Initially, selected process factors are varied at two and three levels using a Taguchi Design of Experiment (DOE) approach to identify robust processing combinations that minimize void formation under nominal lab conditions, as quantified through optical microscopy (OM). Then, the fibre volume fraction of the repair patch is evaluated by applying pyrolysis, with the use of Thermogravimetric Analysis. The results indicate that vacuum-assisted impregnation with the use of Double Volume Debulking bagging configuration yields the least void formation, promoting better repair patch quality.

2. Introduction

Carbon fibre reinforced polymer composite (CFRP) sandwich is increasingly used in primary load-bearing aircraft structures due to its superior material properties and performance. For example, CFRP fuselages provide higher allowable hoop stresses and improved corrosion resistance, enabling higher cabin humidity and pressure levels for passenger comfort [1]. Despite these advantages, CFRP composites remain susceptible to various damage mechanisms during both service (e.g., lightning strikes, debris impacts) and manufacturing (e.g., tool drops during inspection, delamination during production) [2]. Such damage can significantly degrade mechanical properties and compromise structural integrity. When damage is limited, bonded repair techniques can be applied to restore airworthiness by ensuring adequate bond strength and longterm durability. Among current repair methods, step-bonded repairs using wet layup have gained attention as a practical alternative to traditional prepreg scarf repairs, primarily due to shorter curing times and lower processing temperatures [3]. Unlike prepreg repairs, wet layup processes do not require refrigerated storage and can be performed using out-of-autoclave (OOA) consolidation, eliminating the need for autoclaves. In addition, step geometries are generally easier to implement than scarf geometries in terms of tooling and required expertise. The typical bonded repair workflow, from damage assessment to patch application, is summarized in Figure 1 [4].

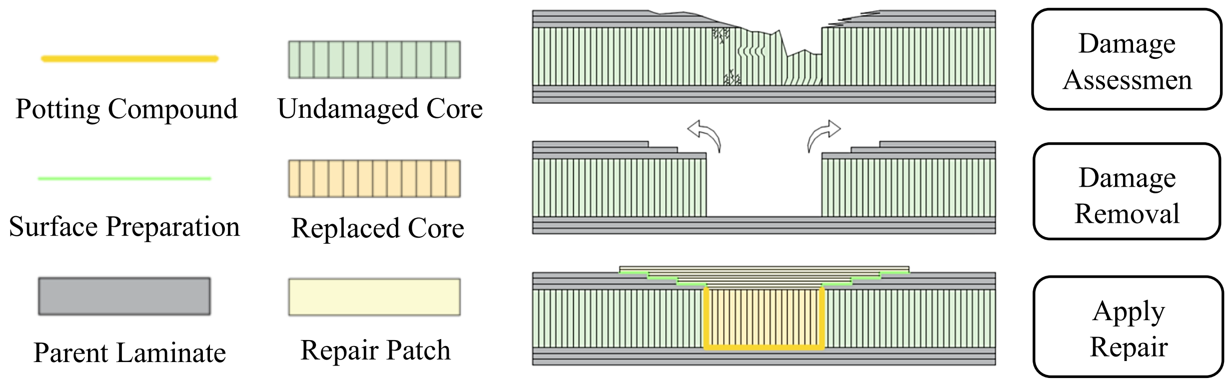

Figure 1 Key stages of step-bonded repair process

However, critical stages of the repair process, specifically the patch fabrication, still face significant challenges. The structural performance of composite repairs is highly dependent on the manufacturing conditions. Proper curing cycles and layup techniques, including fibre placement, resin impregnation, and vacuum bagging, are necessary to produce repair patches with minimal void content [5]. In wet layup repairs, dry fabrics are impregnated with resin directly over the damaged area to reconstruct the laminate. Industrial approaches to reduce void formation include manual resin impregnation and vacuum-assisted impregnation, where fabrics are compacted within a vacuum bag to improve resin distribution and reduce air entrapment [6]. Due to the fact that many aircraft components cannot be removed from service for repair, bonded repairs are typically performed on-site using OOA processing under vacuum bag consolidation. Techniques such as single-sided vacuum bagging or DVD enable efficient repairs of large composite structures [7-8]. The choice of consumable materials within the vacuum bagging arrangement, such as perforated release films, non-perforated release films, and peel plies, can also influence consolidation quality [9].

Nevertheless, bonded repair performance is sensitive to numerous process parameters. Inadequate impregnation or insufficient consolidation pressure can lead to poor patch quality and increased void content. Achieving an optimal fibre volume fraction is critical, as excessive fibre content can limit resin wet-out while insufficient fibre content reduces mechanical performance. Maintaining pressure near atmospheric levels during curing improves resin flow and enhances interfacial adhesion [10]. From these studies [11-13], wet layup bonded repairs in sandwich structures remain relatively underexplored, and the influence of process-induced variations is not yet well defined. In particular, the influence of vacuum bagging configurations, impregnation strategies, and process-induced variability on repair patch quality has not been systematically characterized. This lack of process control guidelines limits the reliability and repeatability of in-service bonded repairs. Therefore, this study aims to develop a systematic wet layup repair methodology for CFRP sandwich structures, focusing on how processing parameters affect patch consolidation and overall repair quality.

3. Methodology

3.1. Materials and Tools

To evaluate repair patch quality, a MIC-6 aluminum mould was manufactured to replicate the parent laminate, enabling easy release of the fabricated patches for quality assessment. The mould incorporates step geometry, and core removal features following damage assessment. The repair patches were fabricated using epoxy resin (LOCTITE EA 9390) and dry fabrics (plain weave T650-35-3k carbon). A NOMEX hexagonal core (12.7 mm thickness) was used as the replacement core, sealing the core with potting compound (LOCTITE EA 9394). The mould assembly was placed on top of a permeability test apparatus to monitor pressure evolution within the core during processing. The repair patch consists of eight plies, including filler and overlay plies, arranged in the stacking sequence $[(0/90)_2 \pm 45/0/90]$ as shown in Figure 2. To simulate on-site repair condition, curing was performed using a heating blanket regulated by a proportional–integral–derivative (PID) controller. The temperature and pressure evolution during processing were recorded using a data acquisition (DAQ) system integrated with LabVIEW.

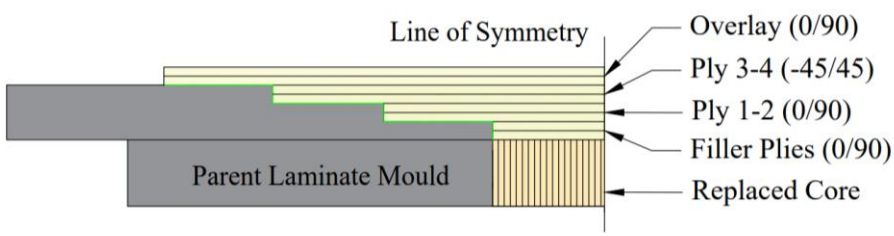

Figure 2 Cross-section schematic of the patch layup configuration over the parent laminate mould

3.2. *Test Matrix*

A key challenge in manufacturing step repair patches with minimal voids lies in the variability of processing parameters. To assess the influence of each parameter, the selected variables were assigned two or three levels in Table 1, where Level 1 represents the industrial baseline configuration. An L18 Taguchi orthogonal array was employed to design the experimental matrix.

Table 1 Design levels of repair patch process parameters

Factor	Description	Level 1	Level 2	Level 3
A	Impregnation	Manual	Random Blob	Vacuum Assisted
B	Bagging arrangement	Single	DVD	-
C	Room Temperature (RT) Debulking duration	120 min	0 min	60 min
D	Perforated release film	P3	P	-
E	Cure Cycle	Slow ramp (2°C/min)	Fast ramp (5°C/min)	Two dwells (2°C/min) with 30 min hold at 60°C
F	Potting Compound	Yes	No	-

Table 2 Taguchi L18 orthogonal array test matrix

	Experimental Trials																	
Factors	1	2	3	4	5	6	7	8	9	10	11	12	13	14	15	16	17	18
A	1	2	3	1	2	3	1	2	3	1	2	3	1	2	3	1	2	3
B	1	1	1	1	1	1	1	1	1	2	2	2	2	2	2	2	2	2
C	1	2	3	2	3	1	3	1	2	3	1	2	1	2	3	2	3	1
D	1	1	1	2	2	2	2	2	2	1	1	1	2	2	2	2	2	2
E	1	3	2	2	1	3	3	2	1	2	1	3	3	2	1	1	3	2
F	1	1	1	2	2	2	2	2	2	2	2	2	1	1	1	1	1	1

3.3. Repair Patch Processing

3.3.1. Core Replacement

The potting compound was mixed according to the manufacturer-specified ratio of Part A to Part B. The quantity of potting compound was calculated to achieve a thickness of 2 mm on the external surface of the replaced core [14]. The compound was first applied to the sides and bottom of the cavity, after which the core was positioned, and the remaining compound was applied to the surface. The assembly was then cured under vacuum with peel ply applied on top, using atmospheric pressure compression at 66 °C for 1 hour. After curing, the core surface was flush-finished using 240-grit sandpaper.

3.3.2. Impregnation

The resin-to-dry-fabric mass ratio was maintained at 1.5:1. The resin was mixed in a plastic container using a wooden depressor and subsequently degassed for 5 minutes. Three impregnation techniques were investigated, as illustrated in Figure 3, manual, random blob, and vacuum-assisted impregnation. In manual impregnation, the resin was applied onto the dry fabrics placed between drawing films and distributed by hand using a roller to ensure fibre wet-out. In the random blob technique, dry fabrics were pre-cut into the repair patch geometry, and resin was randomly deposited on the surface to promote air evacuation during consolidation. In vacuum-assisted impregnation, breathers were positioned around the dry fabrics between drawing films to create air channels, allowing the vacuum to evacuate entrapped air within the fabric layers.

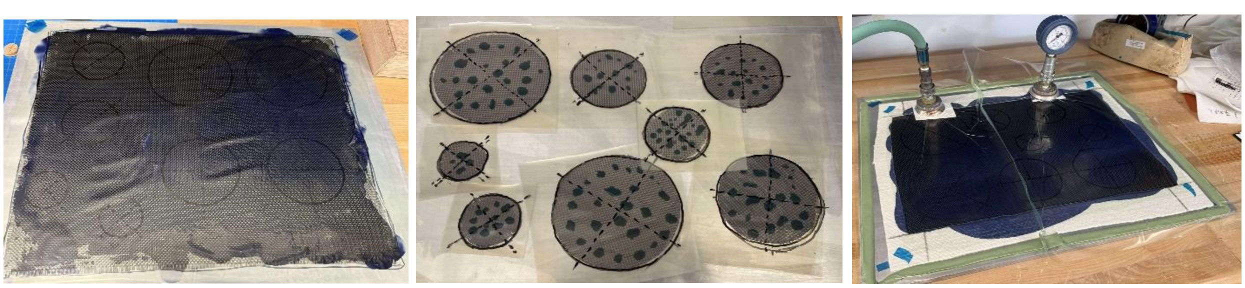

Figure 3 Impregnation techniques (from left to right: manual, random Blob, vacuum-assisted)

3.3.3. *Vacuum Bagging Arrangement*

The vacuum bagging arrangement plays an important role in air evacuation during patch fabrication. A typical single-bag configuration is illustrated in Figure 4. Consumable materials used in the layup included breather/bleeder (to absorb excess resin and protect the vacuum film from heating blanket), perforated release film (to facilitate evacuation of entrapped air), non-perforated release film (to prevent resin bleed into the heating blanket), and vacuum film (for vacuum sealing). Two types of perforated release film were evaluated in the test matrix: P-type with 1.27% open area and P3-type with 0.28% open area. The cure cycle was programmed within the PID controller that regulated the heating blanket, and the copper caul plate was placed underneath the heating blanket to improve the thermal conductivity of the sealed system.

Thermocouples were installed above and below the patch to measure thermal gradients, while the pressure sensor above the vacuum bag monitored the bag's vacuum level. An additional pressure sensor installed in the seal cavity of the permeability test apparatus measured the evolution of vacuum within the core. All thermocouples and pressure sensors were connected to a DAQ system and monitored using LabVIEW.

A DVD configuration was also investigated; this setup utilized two vacuum bags, where the inner bag layup was identical to the single bag configuration. A rigid wooden box was placed over the inner bag to enclose the parent laminate mould, then an outer vacuum bag was made over the box and sealed over the inner bag. The rigid box creates space, preventing the outer bag from collapsing. The process consisted of two stages. Equal vacuum was pulled in both the inner and outer bags during RT debulk. During the debulking stage, the outer bag pressure was maintained at atmospheric pressure (1 atm) while the inner bag remained under vacuum (<1 atm), loosening the inner bag layup and promoting additional air evacuation. Once the cure temperature reached 60 °C, the compaction stage began by venting the outer bag to the atmosphere. This allowed the inner bag pressure to approach atmospheric pressure, resulting in improved consolidation, more uniform patch thickness, and reduced porosity.

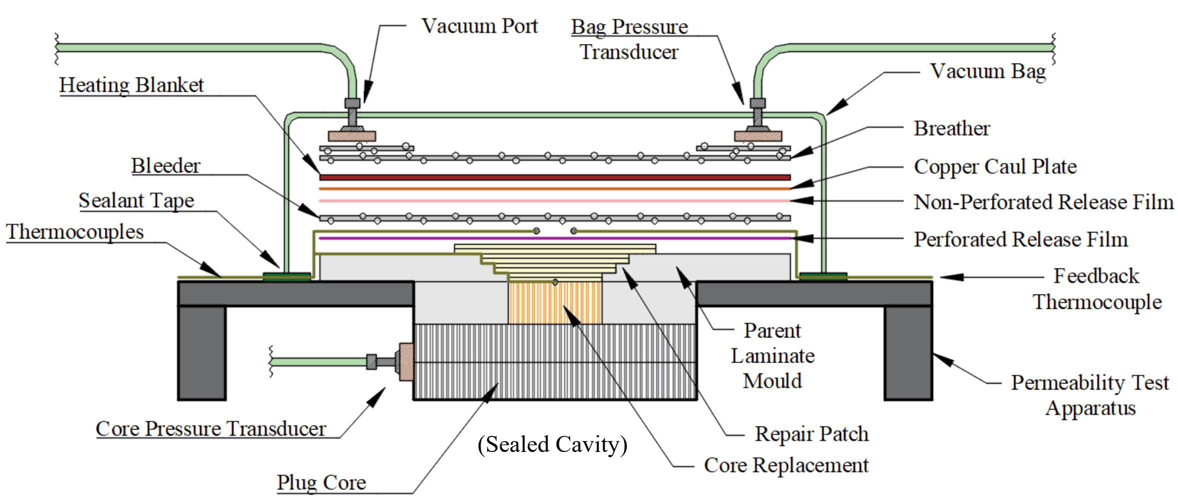

Figure 4 Single bag bleed vacuum bagging arrangements on top of a permeability test apparatus, which is used to monitor gas transport of the core during repair patch processing.

3.3.4. Repair Patch Curing Cycle

Depending on the test matrix, the repair patch was debulked under vacuum for 0–120 minutes before curing. For single-dwell cure cycles, the system was ramped at either 2 °C/min or 5 °C/min to the designated dwell temperature. For two-dwell cycles, an intermediate dwell at 60 °C was introduced for 30 minutes to prolong the period during which the resin remains near its minimum viscosity before ramping at the same rate to the final hold temperature. Finally, the resin was cured at 93 °C for 220 minutes.

3.4. Material Characterization

After curing, the repair patches were removed from the mould and sectioned into small specimens with a diamond saw. Samples were collected from the bonding region between the composite laminate and the honeycomb core, as shown in Figure 5. The specimens were mounted using *Amazing Clear Cast* resin, followed by polishing and examination under OM. The fibre volume fraction was evaluated using Thermogravimetric Analysis (TGA). The resulting mass loss was then used to determine the average patch fibre volume fraction using the rule of mixtures.

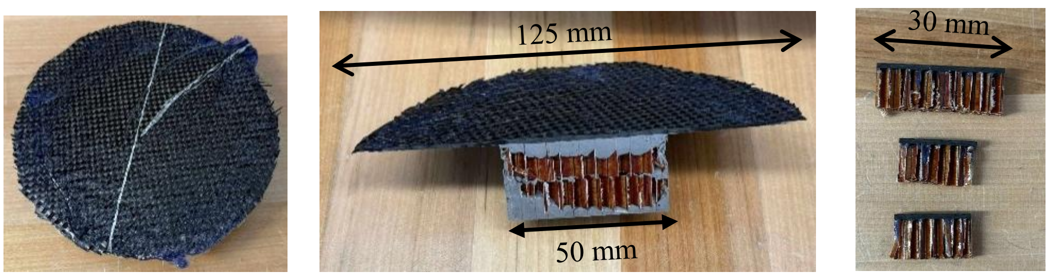

Figure 5 Sample collection (from left to right: repair patch; cross-section; microscopy samples)

4. Results and Discussion

4.1. Void Content

Three samples were collected for each experimental trial. Since the objective of this study is to improve the wet layup repair process with both low void content and good repeatability, the signal-to-noise (S/N) ratio was evaluated for each trial using analysis of variance (ANOVA) [15]. This approach enables simultaneous assessment of process parameters influencing both void content and variability. A wide variation in repair quality was observed across the experiments. The average void content ranged from 1.6% (Trial 18) to 5.2% (Trial 13), with an overall mean of 3.4%. Correspondingly, the S/N ratio varied from 4.3 (Trial 18) to 14.3 (Trial 13).

Only trials that achieved lower void content than the industrial baseline (Trial 1: 2.7%) are shown in Figure 6, with average void content and corresponding standard deviation. Improvements were primarily associated with the use of vacuum-assisted impregnation (Trials 3, 6, 12, 15, 18), the DVD bagging arrangement (Trials 12, 15, 16, 18), and release films with higher perforation levels (Trials 6, 12, 15, 16, 18). However, certain trials showed improved results despite parameters that would typically degrade quality. For example, the absence of potting compound in Trial 6 could allow trapped air within the core to migrate into the patch, potentially increasing void formation.

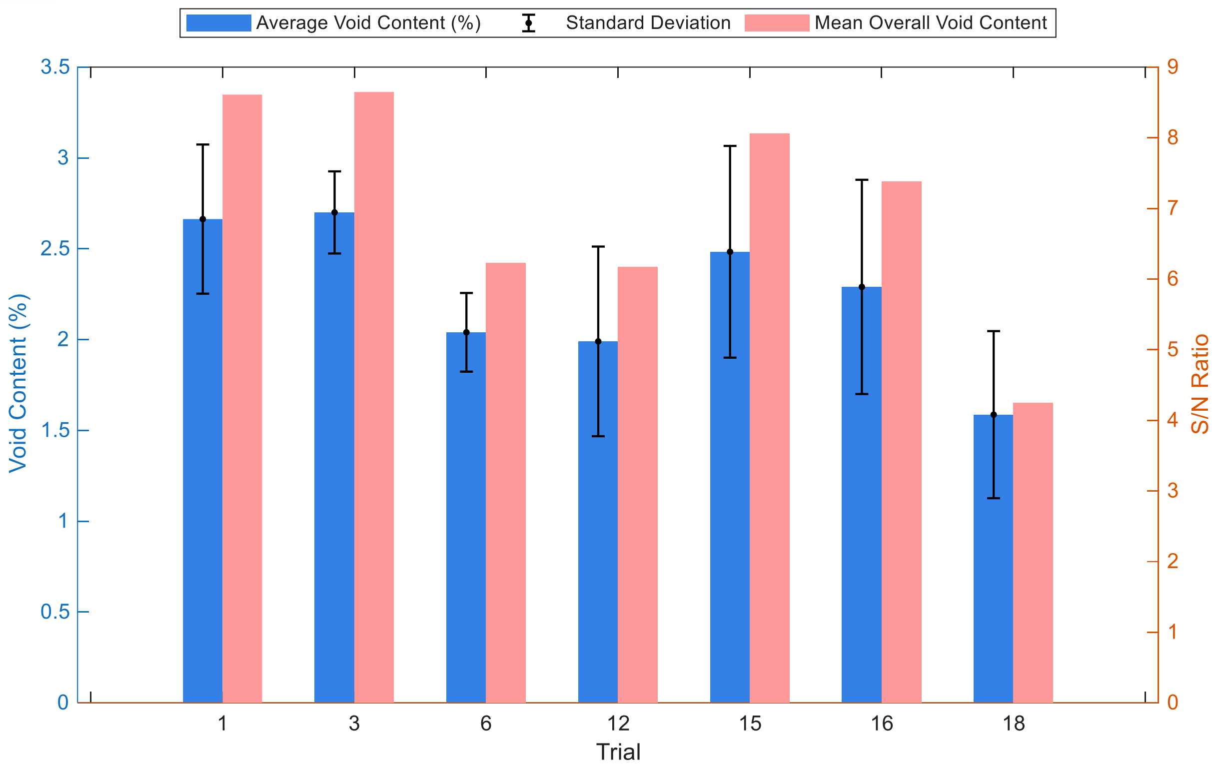

Figure 6 Patch void content and corresponding signal-to-noise ratio for trials with void content lower than the industrial baseline of 2.7%.

To predict the optimal processing conditions among the six parameters, a desirability analysis was performed to minimize both the mean void content and the S/N ratio. The average S/N ratio for each factor at each level was calculated using Equation (1) [13, 15].

$$(S/N)_{avg,Xk} = \frac{L}{n}\left(\sum_{i=1}^{n}\begin{Bmatrix}(S/N)_i, if\ X\ at\ level\ k\\ 0, otherwise\end{Bmatrix}\right) \quad (1)$$

where X defines processing factors (i.e. A, B, C, D, etc.), k denotes the levels of the factor, L is the number of levels, and n is the number of experimental results. The optimal parameter combination predicted by the DOE analysis was not part of the original 18 trials. The optimum configuration includes vacuum-assisted impregnation, DVD bagging arrangement, 120 min room-temperature debulking, P-type perforated release film, a two-dwell cure cycle, and the use of potting compound. A verification experiment was conducted using this optimal configuration, resulting in a minimum void content of 1.50 ± 0.50% with a S/N ratio of 3.95.

Micrographs of the best and worst conditions from the L18 experiments are presented in Figure 7, while Figure 8 shows the corresponding images comparing the industrial baseline with the optimized repair process. Microscopy observations reveal higher porosity in the baseline configuration, particularly with lower-perforation release films, single-bag vacuum arrangements, and manual impregnation. As in Trials 1 and 13, manual impregnation produced greater intra-tow porosity and inter-ply macro-voids. In contrast, the DVD configuration and vacuum-assisted impregnation in Trial 18 resulted in desirable outcomes, improved air evacuation and promoted more uniform ply thickness. The optimized processing conditions reduce void formation through several mechanisms: vacuum-assisted impregnation enhances resin infiltration under atmospheric pressure; DVD bagging improves air evacuation and consolidation; extended debulking and two-dwell cure cycles allow the resin to approach its minimum viscosity and improve flow; potting compound prevents trapped air or moisture within the core from migrating into the repair patch; and higher perforation in release films facilitates air evacuation.

An ANOVA was performed to further identify the most significant processing parameters affecting void content. The results indicate that the impregnation method is the most influential factor, with the highest F-score (6.709) and the lowest p-value (0.01946), demonstrating its statistically significant contribution to void distribution.

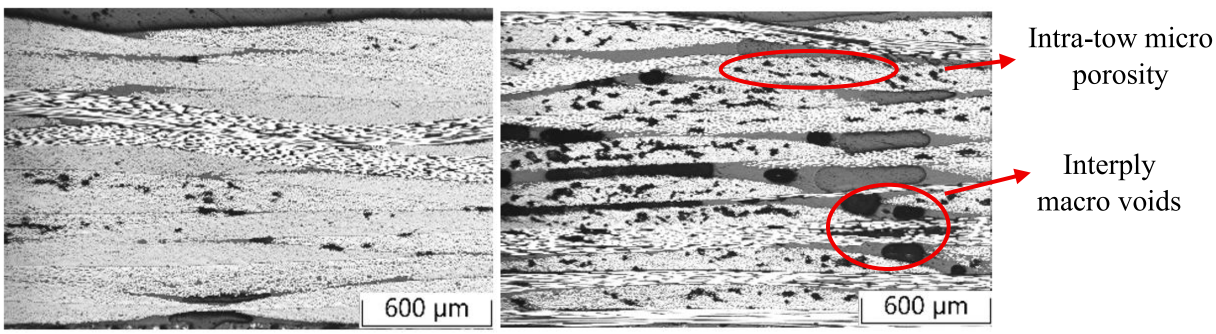

Figure 7 Micrographs comparing the void morphology for the best and worst conditions:
Trial 18, 1.6% - Best (Left), Trial 13, 5.2% - Worst (Right)

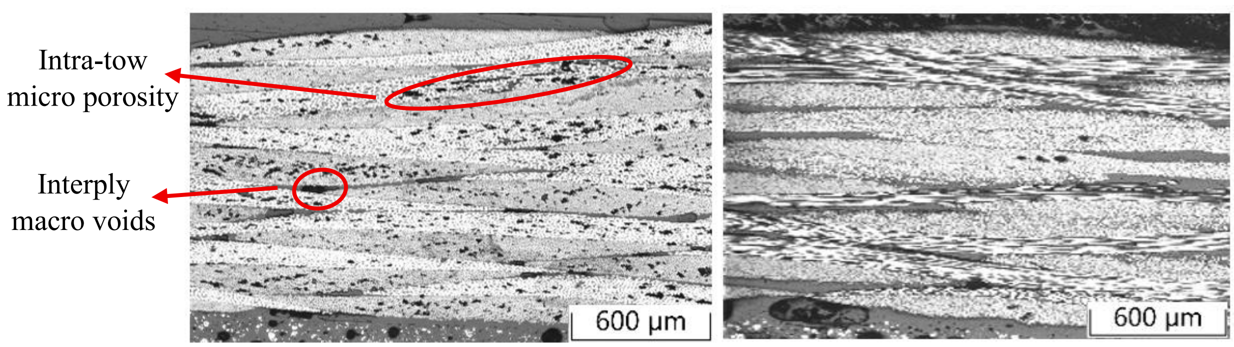

Figure 8 Micrographs comparing the improvements from the industrial baseline condition:
Trial 1 (Baseline), 2.7% - Left, Trial Verification (Optimum), 1.5% - Right

4.2. Fibre Volume Fraction

Across the 18 experimental trials, the fibre volume fraction ranged from 50to 60%, with an average of 56% and a standard deviation of 1.8%. Incorporating the fibre volume fraction results into the ANOVA analysis indicates that Factor D (perforated release film) has the most significant influence on fibre volume fraction. During resin preparation, the resin-to-fibre mass ratio resulted in an initial fibre volume fraction of 24%. Comparison with the final measured fibre fractions shows that approximately 25-30 % of resin was removed during processing when using P3-type and P-type perforated release films, respectively, as summarized in Table 3.

Table 3 Comparison of fibre volume fraction for perforated release film types

Perforated release film	P3 Type (0.27% open area)	P Type (1.27% open area)
Trial number	1-3, 10-12	4-9, 13-18
Fibre volume fraction range	50-53%	57-61%

5. Conclusion

This study developed a systematic approach to improve wet layup bonded repair processes at the laboratory scale. The results show that processing parameters strongly influence repair quality and void formation. The use of vacuum-assisted impregnation, DVD bagging arrangement, longer debulking time, and highly perforated release films significantly reduced both micro- and macro-voids in the repair patches. This study developed a systematic approach to improve wet layup bonded repair processes at the laboratory scale. DOE and ANOVA analysis identified impregnation method as the most significant factor affecting void content, while the perforated release film had the greatest influence on fibre volume fraction. The optimized processing conditions predicted by the DOE resulted in a minimum void content of 1.50 ± 0.50%, which is lower than the current industrial baseline. Overall, the proposed processing strategy improves the quality and repeatability of wet layup repairs and provides useful guidance for composite bonded repair applications.

6. Acknowledgement

The authors would like to acknowledge the financial support and materials from the Consortium for Research and Innovation in Aerospace in Quebec (CRIAQ); the Natural Sciences and Engineering Research Council of Canada (NSERC); the Centre de Recherche sur les Systèmes Polymères et Composites à Haute Performance (CREPEC); Bombardier Aerospace; Pratt Whittney Canada, Delastek, L3-MAS, and Comtek. The authors would also like to thank Henkel Aerospace for donating the resins, and Bombardier Aerospace for donating the plain weave carbon fabric used in this work.

7. References

[1] K. B. Katnam, L. F. M. Da Silva, and T. M. Young, “Bonded repair of composite aircraft structures: A review of scientific challenges and opportunities,” *Prog. Aerosp. Sci.*, vol. 61, pp. 26–42, Aug. 2013, doi: 10.1016/j.paerosci.2013.03.003.

[2] A. Katunin, K. Dragan, and M. Dziendzikowski, “Damage identification in aircraft composite structures: A case study using various non-destructive testing techniques,” *Compos. Struct.*, vol. 127, pp. 1–9, Sep. 2015, doi: 10.1016/j.compstruct.2015.02.080.

[3] R. B. Heslehurst, *Engineered repairs of composite structures*, First edition. Boca Raton: CRC Press, Taylor & Francis Group, 2019.

[4] E. Chesmar, W. Cole, F. Museux, and K. Armstrong, *Care and Repair of Advanced Composites*. 2020. doi: 10.4271/9780768093179.

[5] C. Zhang *et al.*, "Technology roadmap for composite joining and repair," *Compos. Part B Eng.*, vol. 293, p. 112132, Mar. 2025, doi: 10.1016/j.compositesb.2025.112132.

[6] SAE International, "ARP 5319 Impregnation of Dry Fabric and Ply Layup." Aerospace Recommended Practice, 2011.

[7] SAE International, "ARP 5143 Vacuum Bagging of Thermosetting Composite and Metalbond Repairs." Aerospace Recommended Practice, 2023.

[8] H. M. Chong, Z. A. Wu, S. P. Ng, A. S. Subramanian, T. Liu, and S. Feih, "Influence of double vacuum debulking process on co-cured soft-patch carbon fibre composite repairs," *Compos. Part B Eng.*, vol. 168, pp. 367–374, Jul. 2019, doi: 10.1016/j.compositesb.2019.03.051.

[9] Y. Mujahid, N. Sallih, M. Mustapha, M. Z. Abdullah, and F. Mustapha, "Effects of Processing Parameters for Vacuum-Bagging-Only Method on Shape Conformation of Laminated Composites," *Processes*, vol. 8, no. 9, p. 1147, Sep. 2020, doi: 10.3390/pr8091147.

[10] Federal Aviation Administration (FAA), *Aviation Maintenance Technician Handbook - Airframe*. US Department of Transportation, 2023.

[11] M. Préau and P. Hubert, "Processing of co-bonded scarf repairs: Void reduction strategies and influence on strength recovery," *Compos. Part Appl. Sci. Manuf.*, vol. 84, pp. 236–245, May 2016, doi: 10.1016/j.compositesa.2016.01.016.

[12] Sp. Pantelakis and K. I. Tserpes, "Adhesive bonding of composite aircraft structures: Challenges and recent developments," *Sci. China Phys. Mech. Astron.*, vol. 57, no. 1, pp. 2–11, Jan. 2014, doi: 10.1007/s11433-013-5274-3.

[13] A. Maclean, "Experimental Validation of New Vacuum Bag Only Processing Techniques for Co-bonded Composite Repairs," *MSc Dep. Mech. Eng. McGill Univ. Can.*, 2017.

[14] SAE International, "ARP 4991 Core Restoration of Thermosetting Composite Components." Aerospace Recommended Practice, 2014.

[15] D. C. Montgomery and G. C. Runger, *Applied Statistics and Probability for Engineers*, 7th ed. Wiley, 2018.